Thermal Transport in Disordered Materials

A thesis proposal by

Jason M. Larkin

April 25, 2008

224 Scaife Hall

Department of Mechanical Engineering

Carnegie Mellon University

Thesis Committee

Associate Professor Alan McGaughey (Committee Chair), Mechanical Engineering

Professor Jonathan A. Malen, Mechanical Engineering

Professor Michael Widom, Physics

Professor Craig Maloney, Civil and Environmental Enginering

Contents

1 Introduction

1.1 Thermal Transport in Ordered Materials

1) Understanding thermal transport in crystalline systems requires detailed knowledge of the phonon properties.

Thermal transport in a semiconductor is controlled by phonons, quanta of energy associated with atomic vibrations. The properties of phonons are controlled at atomic-level length scales of 0.1-1 nm. Phonons themselves are non-localized vibrations which can extend over 100 nm 10 microns in common semiconducting materials like silicon and germanium. A nanostructured material can be described by an effective thermal conductivity, which can be very different than the bulk values available in common references. The effective thermal conductivity of a nanostructure is lower than the bulk value due to the scattering of phonons with the system boundaries which have length scales of 10 nm 100 microns.

1.2 Thermal Transport in Disordered Materials

2) Thermal transport in dilute alloys should have significant contribution from phonons. As the alloy concentration is increased, the vibrational modes should become localized and non-propagating.

1) Thermal transport in amorphous materials is typically modeled as completely localized vibrations which propagate diffusively.[3] This diffusive propagation is much slower than the long-range propagation of phonons, and thus the thermal conductivity of amorphous materials is typically several orders of magnitude less than crystalline systems.[5,14]

The first evidence of such localized modes, was reported by Keppens et al.[1] using heat capacity, elastic constant and inelastic neutron-scattering measurements. They were able to explain their heat-capacity data with the Debye model plus two fitted Einstein oscillators. Recently there have been debates on this picture. It has been pointed out by a higher resolution neutron scattering that the previously observed peaks were due to van Hove singularities, that is, optical phonons and zone boundary modes.

1) Thermal transport in amorphous materials has AF theory, but recent measurements show that this theory is incomplete because it does not consider the contribution from phonons to thermal transport.[?] These modes are long wavelength and thus sample an effective medium of the underlying disordered atomic structure.

1) The AF theory of thermal transport in amorphous solids also does not consider the effects of anharmonicity, which will be inverstigated using a combination of MD and LD calculations.[6]

1) what do ab initio structures/calculations predict for amorphous materials, such as silicon? Use DFT MD to produce amorphous structure(s). Use harmonic FC's to run classical MD and Green-Kubo. Is it possible to accurately predict thermal conductivity using harmonic FCs for other disordered systems such as alloys?

Predicting and describing transport physics requires insight into the movement and scattering of transport carriers. Transport carriers include fluid molecules, electrons, and phonons (quantized lattice vibrations).[18] These carriers are what move in response to spatial gradients and give rise to mass, momentum, charge, and thermal energy fluxes through a system. The carriers available for transport are directly related to the chemical composition and thermodynamic phase of the host material. For example, heat flux through crystalline solids is realized by phonons (in an electrically insulating crystal) or electrons (in an electrically conducting crystal). In an ideal gas, heat flux is realized by elastic collisions between atoms and molecules.

1.3 Large Unit Cell Materials for Thermoelectric Energy Generation

Thermoelectric energy generation - the transformation of waste heat into useful electricity - is a promising source of sustainable energy.[13] Thermoelectric materials directly convert temperature differences into electric voltage as a result of their intrinsic (atomic-level) electronic and thermal properties. The performance of a thermoelectric device can be quantified through the thermoelectric figure of merit, ZT = , where T is the average device temperature, S is the Seebeck coefficient (the ratio of the induced thermoelectric voltage to the applied temperature difference), is the electrical conductivity, and is the thermal conductivity. For thermoelectric devices to be competitive with traditional power generation cycles requires ZT ¿ 3.[9] Achieving this performance is challenging because the electrical and thermal properties in ZT are coupled in the majority of materials.[9,13] The ideal thermoelectric can be thought of as an electron-crystal/ phonon-glass (high , low) (see Figure 1). Reducing has become a primary strategy in the design of new thermoelectric materials.[13] Using nanostructuring to reduce while maintaining good electrical properties has been identified as one possible strategy,[26] but such materials are costly. An emerging area of study in thermoelectric power generation is the use of large unit cell (LUC) crystals.[13]

Large unit cell crystals have an ordered (crystalline) structure, but the basic building block (unit cell) of the crystal has a large number of distinct atoms (Figure 1).[17,38,39] They are effectively disordered over length scales on the order of the atomic spacing and their thermal conductivities can be as low as a glass.[17,38,39] The key advantage of LUC materials

is that they are still ordered from the standpoint of electrons, which results in large and ZT. Thus, LUC crystals are electron-crystal/phonon-glass materials. Current LUC crystals have ZT¡3[17,38,39] and more research is required to improve their thermoelectric performance. The LUC crystals to be studied here are skutterudites[17] and Zintl compounds[38] (Figure 2). Both of these LUC crystals have , but experimental measurements show intriguing potential for improved thermoelectric efficiency.[17,38,39]

It is likely that the thermoelectric performance of large unit cell materials has yet to be fully realized.

1.4 Zeolites for Gas Adsorbation

The porous crystals are a diverse group of materials characterized by large unit cells and Angstrom sized pores and channels. Among these are the zeolites [1], skutteru- dites [2], fullerenes [3], and metal organic frameworks [4,5]. The size of the pores is on the same scale as the dimensions of many atoms and molecules, leading to the use of porous crystals as molecular sieves and catalysts, and for gas storage applications.

There is also interest in the design of porous crystals with very low thermal conductivities for applications as rigid insulators and to protect stored gases from ambient temperature fluctuations. As a first step towards design for thermal properties, the mechanisms by which heat is transferred in these materials must be understood. Here, this goal is pursued in the context of the zeolites.

Which phonons/vibrational modes are affected by the adsorbed gas molecules? Cite Thomas CNT/water study for possible scattering. In these zeolite systems, modes may not be phonons. Possibly need to study the time scale you can extract from the AF calculation.

1.5 Amorphous Materials

Amorphous materials are used in a number of applications:

- Amorphous silicon solar cells
- amorphous silicon/silica substrates for various applications

  cite measurements of anomlalous high amorphous thin film conductivity
- amorphous metals, which are most likely still dominated by electron thermal/electrical transport.

1.6 Research Plan

The objectives of the proposed research are to:

- Investigate thermal transport in crystals, alloys, and amorphous samples using model LJ systems.
- Develop methodology to identify relative contribution to thermal transport from thermal diffusivities in these systems.
- Design and perform ab initio simulations to predict the thermal properties of realistic LUC crystals.

2 Thermal Transport in Ordered and Disordered Materials

Thermal Conductivity in Ordered Materials

$$k_{thermal} = \&k_{elec} + k_{lattice} = \&k_{lattice} \tag{1}$$

$$k_{elec} = \tag{2}$$

Making no assumptions about the phonons, the lattice thermal conductivity is given as a sum over all phonon modes with mode specific properties

$$k_{lattice,\mathbf{n}} = \sum_{\boldsymbol{\kappa}} \sum_{\nu} c_{ph}(\boldsymbol{\kappa}_{\nu})\, v^2_{g,\mathbf{n}}(\boldsymbol{\kappa}_{\nu})\, \tau(\boldsymbol{\kappa}_{\nu})\,. \tag{3}$$

Taking the specific heat to be $c_{ph}(\boldsymbol{\kappa}_{\nu}) = k_B$, the thermal conductivity is

$$k_{lattice,\mathbf{n}} = \sum_{\boldsymbol{\kappa}} \sum_{\nu} k_B D(\boldsymbol{\kappa}_{\nu})\,. \tag{4}$$

And the thermal conductivity is determined by the phonon mode diffusitivies,

$$D(\boldsymbol{\kappa}_{\nu}) = (\boldsymbol{\kappa}_{\nu})\, v^2_{g,\mathbf{n}}(\boldsymbol{\kappa}_{\nu})\, \tau(\boldsymbol{\kappa}_{\nu})\,. \tag{5}$$

Using the Debye model, the thermal conductivity can be re-written

$$k_{lattice} = \frac{1}{3}\int_0^{\omega_D} C(\omega) D_p(\omega) d\omega. \tag{6}$$

$$D_p(\omega) = v^2(\omega)\tau(\omega). \tag{7}$$

2.1 Phonon Lifetimes and Scattering Mechanisms

$$\frac{1}{\tau} = \frac{1}{\tau_{p-p}} + \frac{1}{\tau_b} + \frac{1}{\tau_d} \tag{8}$$

$$\tau_{p-p} = (6\pi^2)^(1/3)/2Mavgv_g v_p^2/V^1/3\omega^2\gamma^2 T \tag{9}$$

$$\tau_b = L/v_g \tag{10}$$

$$\tau_d = \frac{V\omega^4}{4\pi v_p^2 v_g}(\sum_i c_i(1 - m/\bar{(}m_i))^2 + \sum_i c_i(1 - r/\bar{(}r_i))^2) \tag{11}$$

Thermal Conductivity in Disordered Materials

2.2 Phonons in Disordered Materials

2.3 Dilute Alloys

$$k_{lattice} = k_{phonon} \tag{12}$$

$$\tau_d = \frac{V\omega^4}{4\pi v_p^2 v_g}(\sum_i c_i(1 - m/\bar{(}m_i))^2 + \sum_i c_i(1 - r/\bar{(}r_i))^2) \tag{13}$$

Phonons still dominate the transport:

$$\frac{1}{\tau} = \frac{1}{\tau_{p-p}} + \frac{1}{\tau_b} + \frac{1}{\tau_d} \tag{14}$$

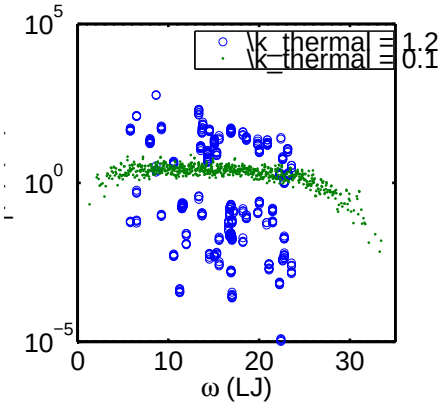

Figure 1: plot comparison of phonon diffusivity versus AF mode diffusivity for LJ 4x.

2.4 High Concentration Alloys and Glasses

Alan 2004 IJMHT amorphous silica shows increasing k with T in classical system, not a heat capacity effect.

$$k_{lattice} = k_{phonon} + k_{AF} \tag{15}$$

$$k_{AF} = \sum_i C(\omega_i)_i D(\omega_i)_i \tag{16}$$

Given Fig. 1, how can we differentiate between phonons and AF modes? Galli says it's when the phonon mean free path is on the order of the atomic spacing. However, it seems more appropriate to consider the AF or phonon mode diffusivities. For example, some phonon modes have a finite lifetime, but vanishing group velocities.

Cahill[7] suggests that the phonon mean free paths in glasses scales as the wavelength of the mode:

$$l_{glass} = \lambda/2 \tag{17}$$

This length scale is still much larger than atomic spacings! Galli suggests that the differentiation between phonon and AF modes is when the phonon mean free path is on the order of the atomic spacings.

Cahill model leads to following scaling of lifetimes in glasses[7]

$$\tau_{glass} = \pi fracp\omega \tag{18}$$

Hypothesis:

May be more likely that the low frequency acoustic phonons in glasses follow a Debye model with Umklapp scattering:

$$\tau_{p-p} = (6\pi^2)^(1/3)/2Mavgv_g v_p^2/V^1/3\omega^2\gamma^2 T \tag{19}$$

Under this hyopthesis, the lattice thermal conductivity from phonons is

$$k_{phonon} = \frac{(6\pi^2)^(2/3)}{4\pi^2}\frac{Mavgv_s^3}{V^{2/3}\omega^2\gamma^2 T} \tag{20}$$

Which can be accounted for using Lattice Dynamics. If this result for the phonon contribution can be combined with the AF contribution, then disordered materials can characterized solely from (harmonic) lattice dynamics which is computationally inexpensive (see Appendix **??**).

2.4.1 AF Lifetime

Using dimensional analysis, the thermal diffusivity calculated by the AF theory can possibly be decomposed into a velocity and time scale:

$$D(\omega_i)_i = v_{AF}^2 \tau_{AF} \tag{21}$$

Figure 2: Plot [100] dispersion w(k,c=0..0.5) showing **effectivemass** effect and N effect

Figure 3: Plot [100] dispersion of 4x crystal using supercell definition, c=0.5, amorphous

3 Controlling Thermal Transport in Disordered Materials

3.1 Controlling Thermal Transport by Dispersion

Controlling dispersion through

- mass ratio

  k is dramatically overestimated by the Debye model when mass contrast is high (e.g. BaO, mass ratio of 8.6).[34]

  when limited by Umklapp scattering, the spectral thermal conductivity, $ks(\omega)$, is proportional to $vg(\omega)^2$.

  The relationship between mass contrast and k can be understood by examining the BvK phonon dispersions for a diatomic chain with varying mass ratio, m1/m2. When the mass ratio is low, the Debye model assumption of a constant phonon velocity is reasonable. However, this assumption breaks down as the mass ratio increases and the optical branch flattens.[32]

- Numer of atoms in unit cell

  Generically folds the dispersion branches in, decreasing both acoustic group velocities and flattening optical branches.

- amorphization

  Amorphous sample should be lower coordinated than crystal. This will make the sample bulk modulus smaller, which should lead to a smaller sound speed (acoustic group velocity):

$$v_s = \sqrt{B_{glass}/\rho} \tag{22}$$

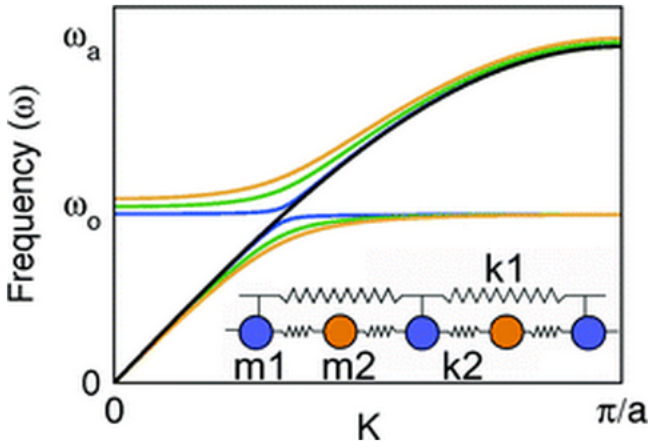

Figure 4: flattening of dispersion .

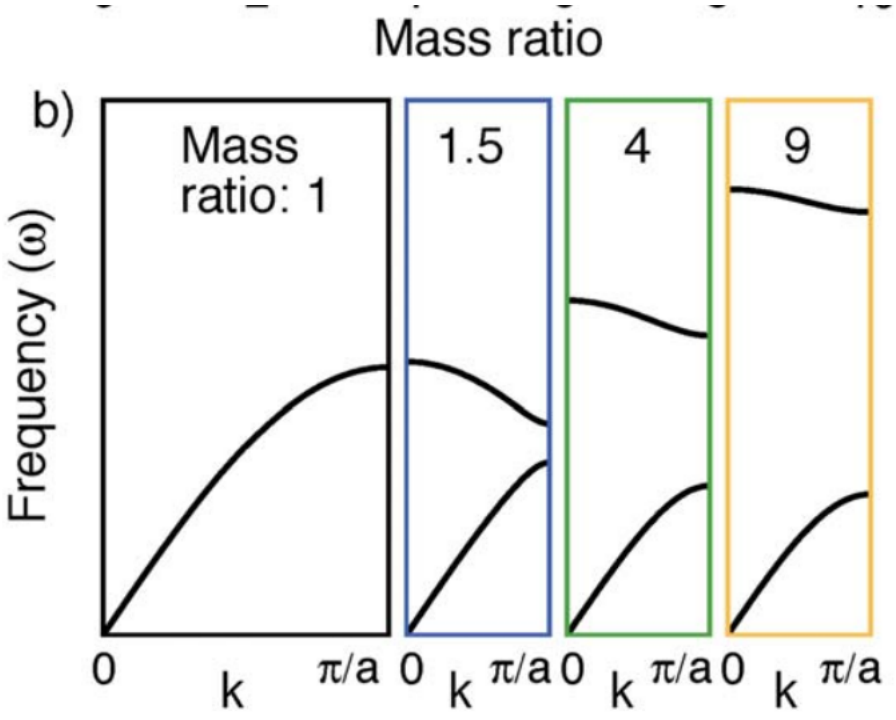

Figure 5: The phonon spectral energy density (Φ) .

Figure 6: NMD unit cell projection c=0..0.15 4x-6x-8x-10x. NMD full cell projection c=0.15 and 0.5 4x-6x-8x-10x.

3.2 Implications for LUC

- Mass Ratios in Diatomic Alloy such as PbTe, Bi2Te3, etc.
- Number of atoms in unit cell effect on group velocity

  As b increases, the phonon dispersion folds in on itself, resulting in b-1 optical modes with low v_g.

  Specifically, the breakdown of the $k = b^{-2/3}$ (Umklapp dominated) or $k = b^{-1}$ (boundary scattering dominated) scalings need to be investigated. This implies that sub-unit cell effects are important since the scalings rely on phonons to develop those scalings.

3.3 Controlling Thermal Transport by Thermal Diffusivity

$$D_p = \tau p - p v_g^2 \tag{23}$$

Boundary scattering attacks the low frequency/long wavelength modes, defect scattering attacks the high frequency/short wavelength, and Umklapp scattering attacks the mid-low frequency/intermdiate wavelength modes.

AF modes have much smaller diffusivity than the dominant diffusivities above (when present):

$$D_{AF} = \tau AF v_{AF}^2 \tag{24}$$

In other words, the design strategy is to minimize the other diffusivities and so that only D_{AF} remain. How are the D_{AF} controlled?

- bonding/coordination. This may be where the Si02 measurements can come in
- quench rates, etc. Do not want to investigate this.
- nanostructuring to beat the "amorphous limit", WSe2, etc.

3.4 Thermal Diffusivity Implications for LUC

3.4.1 b=∞ Large Unit Cells and Allen Feldman Modes

At the amorphous limit ($N = \infty$), the acoustic contribution (ka) approaches zero, whereas in practice, glasses still possess finite thermal conductivity.

Clearly, we cannot completely ignore the thermal conductivity of the optical modes in which most of the heat in a complex solid is stored. As a lower bound to the optical contribution to thermal conducivity (ko), one can look to Einsteins treatment of heat transport as the diffu- sion of heat between atomic oscillators.

Cahill

$$l_{glass} = \lambda/2, \tag{25}$$

This is still much larger than distance between atoms!**?** Allen Feldman modes are D_i

Cahill model leads to following scaling of lifetimes in glasses[7]

$$\tau_{glass} = \pi fracp\omega \tag{26}$$

How do these models agree in limits? Why is this a good model, because it fits data? This represents a clear difference between theoritical and empirical modeling. Does amorphous NMD calculate phonons with lifetimes which follow this trend? If not, then this model's only purpose is to provide fitting parameters to fit empirical data.

4 Large Unit Cell Materials

4.1 SiO2

How is this a model system for LUC?

Is it based on N=small, but many configurations. The different configurations must give different thermal conductivities. Quantify phonons and AF contributions.

Show that there is more scattering for some given coordiantions, indicating the importance of bonding/coordination in a control system. If this is true, should be able to show this in an AF calculation in therms of the diffusivities.

Might be alot easier to show this than do a phonon calculation.

Denisty probably changes though, so figure out a way to possibly collapse the data.

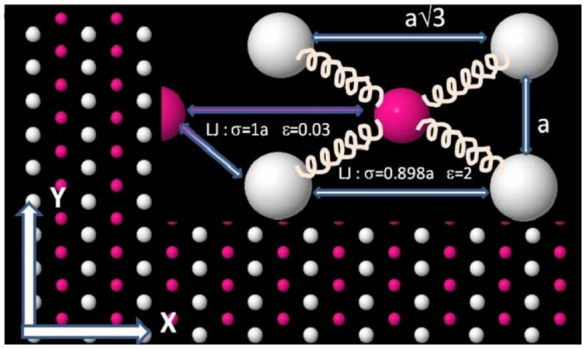

Figure 7: The phonon spectral energy density (Φ) .

4.2 Skutterudite Materials

List the design strateiges presented above which can study these systems:

4.2.1 Rattling Modes

Much of the excitement surrounding skutterudites and clathrates has been focused on the prediction66 and observa- tion of a phenomena termed rattling, observed when the guest atom is under-constrained and weakly bound.[1,10,30]

Experimentally, materials in which guest atoms are strong rattlers are found to exhibit extremely low kL.[28,30] While it is widely accepted that rattling atoms result in strongly localized modes within the acoustic frequency range, the mechanism by which rattler modes reduce kL is under debate.

The reduction in kL has been attributed to resonant scattering by the guest atom.[11] However, the impact of rattling on the group velocity has recently been recognized as an alternative explanation of the low experi- mental kL.[2,39]

used to explain the unusual temperature dependence of kL for both clathrates and skutterudites.71,76 However, these models assume a constant group velocity, which fails to capture the complexity of the phonon dispersion and the interaction of the rattling and acoustic modes.

Fleurial et al.2 experimentally showed that the thermal conduc- tivity decreases exponentially as the atomic-displacement parameter increases.18

18 C. Godart, A. P. Gonalves, E. B. Lopes, and B. Villeroy, Prop- erties and Applications of Thermoelectric Materials Springer, Netherlands, 2009.

4.3 Zeolites for Gas Adsorbation

5 Outcomes and schedule

The outcomes of this proposed research will be:

- Characterization of Thermal Transport in Disordered Materials using LJ Models
- Investigation of Thermal Transport in Large Unit Cell Materials
- Investigation of Harmonic and Anharmonic Contributions to Thermal Transport in Disordered Materials
- Computational Cost Analysis of Harmonic and Anharmonic Calculations
- Detailed Computational Framework

The schedule for my proposed research is provided in Table:

Task	Fall 2011	Winter 2012	Spring 2012
Characterization of Disordered LJ Models	———	———	
Investigate Harmonic and Anharmonic Contributions			———
Task	**Summer 2012**	**Fall 2012**	**Winter 2013**
Investigate Transport in LUC	———	———	
Investigate Transport in LUC using Ab-Initio			———
Investigate Harmonic and Anharmonic Contributions			———
Task	**Spring 2013**	**Summer 2013**	
Si amorphous study using Ab-Initio	———		
Deliver thesis		———	———

6 Biographical Sketch

Jason Larkin was born in Monroeville, PA. He obtained his Bachelor's of Science degree in mechanical engineering from the University of Pittsburgh in Spring 2007. He obtained his Master's of Science degree in mechanical engineering in summer 2009 with a thesis: Statistics of Particle Concentrations in Free-Surface Turbulence. He entered Carnegie Mellon in Fall 2009 where he is pursuing his PhD in mechanical engineering.

Awards

Northrop-Grumann Fellow, CIT Institute for Complex Engineered Systems (ICES) 2011

NSF Graduate Student Research Grant, University of Pittsburgh Department of Physics 2007-2009

2011 Bennett Presentation (Award for Best Presentation).

October 2011 Cover article for Physics of Fluids.

Peer-reviewed Journal Publications

- Predicting Phonon Properties of Silicon from First -Principles Calculations, A. Jain, J.M. Larkin, A.J.H. McGaughey, W.A. Al-Saidi, in preparation.
- Predicting Phonon Properties of Disordered Systems, J.M. Larkin, A.J.H. McGaughey, Ankit Jain, in preparation.
- S. Stefanus, J. Larkin, W. Goldburg, A Search for Conformal Invariance in Compressible Two Dimensional Turbulence, Physics of Fluids 23 (2011) 105101. Selected for cover.
- J. Larkin, W. Goldburg, M.M. Bandi, Time-Evolution of a fractal distribution: Particle concentrations in free-surface turbulence, Physica D 239 14 (2010) 1264-1268.
- J. Larkin, W. Goldburg, Decorrelating a Compressible Turbulent Flow: an Experiment, Physical Review E 82, 016301 (2010).
- J. Larkin, M.M. Bandi, A. Pumir, W. Goldburg , Power -law distributions of particle concentration in free-surface flows, Physical Review E 80, 066301 (2009).

Conference Presentations

1. Predicting Phonon Properties of Silicon from First -Principles Calculations, J.M. Larkin, A.J.H. McGaughey, W.A. Al-Saidi, to be presented at 2012 ASME Summer Heat Transfer Conference Puerto Rico, USA.

2. Comparison of Spectral Energy Methods for Predicting Phonon Properties, J.M. Larkin, A.D. Massicotte, J.E. Turney, C.H. Amon, A.J.H. McGaughey, to be presented at 2012 ASME Micro/Nanoscale Heat & Mass Transfer International Conference Atlanta, GA.

3. Predicting Thermal Conductivity of Defected Systems using the Spectral Energy Density, J. Larkin 2011 MRS Fall Meeting Boston, MA.

4. Predicting Thermal Conductivity of Defected Systems using the Spectral Energy Density, J. Larkin 2011 Bennett Presentation (Award for Best Presentation).

5. Decorrelating a Compressible Turbulent Flow: An Experiment, J. Larkin, W. Goldburg (speaker), 2010 American Physical Society March Meeting Portland, OR.

6. Statistics of Preferential Particle Concentration in Free -Surface Turbulence, J. Larkin (speaker), M.M. Bandi, W. Goldburg, 2009 American Physical Society March Meeting Pittsburgh, PA.

7. Experimental Determination of the von Karman Constant in Turbulent Two Dimensional Soap Film Flows, Nicholas Guttenberg (speaker), Nigel Goldenfeld, Jason Larkin, Alisia Prescott, Hamid Kellay, Walter Goldburg, 2008 Meeting of the APS Division of Fluid Dynamics San Antonio, TX.

8. Turbulent Dynamics of a Hydraulic Jump in two dimensions: Soap Film Flow Jason Larkin (speaker), Walter Goldburg, Tuan Tran, Pinaki Chakraborty, Gustavo Goia, 2008 Meeting of the APS Division of Fluid Dynamics San Antonio, TX.

9. The Generalized Fractal Dimensions of a 2 -D Compressible Turbulence, J. Larkin (speaker), M.M. Bandi, W. Goldburg, 2008 American Physical Soci ety March Meeting New Orleans, LA.

10. Design of a Flow Chamber to Explore the Initiation and Development of Cerebral Aneurysms, Jason Larkin, John P. Barrow, A. M. Robertson 2007 Biomedical Engineering Society Meeting Undergraduate Presentation Los Angeles, CA

7 MISC

For LUC systems, are the barriers more important than the crystallinity?

2) Rigidity-percolation models?

Feng Sen, Sahini Thorpe, Duxbury Boolchand

a) can you just run a harmonic FC MD to measure the conductivity?

Lattice Dynamics

.1 Crystal Energy

expansion of the crystal energy to motivate

.1.1 Lennard-Jones Potential

possibly present LJ, comment that it is simple but anharmonic

.2 Harmonic Approximation and Normal Modes

Show the dynamical matrix, here is where you get eigenvectors/freqs.

.3 Normal Modes in Ordered Solids

start with the real space atomic velocities as represented by the normal mode decomposition,

12

$$\dot{u}_\alpha(\begin{smallmatrix} l \\ b \end{smallmatrix};t) = \sum_{\boldsymbol{\kappa}',\nu}^{N,3n} \frac{1}{\sqrt{m_b N}} \exp\Big[i\boldsymbol{\kappa}' \cdot \mathbf{r}_0(\begin{smallmatrix} l \\ 0 \end{smallmatrix})\Big] e^*\big(\begin{smallmatrix} \boldsymbol{\kappa}' & b \\ \nu & \alpha \end{smallmatrix}\big)\, \dot{q}\big(\begin{smallmatrix} \boldsymbol{\kappa}' \\ \nu \end{smallmatrix};t\big)\,. \tag{27}$$

.4 Phonon Lifetimes from Normal Mode Decomposition

Can get:

$$\tau_{p-p} = (6\pi^2)^(1/3)/2Mavgv_g v_p^2/V^1/3\omega^2\gamma^2 T \tag{28}$$

and for dilute alloys:

$$\tau_d = \frac{V\omega^4}{4\pi v_p^2 v_g}(\sum_i c_i(1-m/\bar{(}m_i))^2 + \sum_i c_i(1-r/\bar{(}r_i))^2) \tag{29}$$

.5 Allowed Wavevectors in Ordered Systems

The phonon spectral energy is defined for the allowed wavevectors of a crystal, which can be specified from the crystal structure's Bravais lattice and its basis, i.e. unit cell. A D-dimensional Bravais lattice is a collection of points with positions

$$\mathbf{r}_0(\begin{smallmatrix} l \\ 0 \end{smallmatrix}) = \sum_{\alpha}^{D} N_\alpha \mathbf{a}_\alpha \tag{30}$$

where N_α and the summations if over the lattice vectors, $\mathbf{a}_\alpha$.[4] The basis (or unit cell) is the building block of the crystal and they are arranged on the points defined by the Bravais lattice. The equillibrium position of any atom in the crystal can be described by

$$\mathbf{r}_0(\begin{smallmatrix} l \\ b \end{smallmatrix}) = \mathbf{r}_0(\begin{smallmatrix} l \\ 0 \end{smallmatrix}) + \mathbf{r}_0(\begin{smallmatrix} 0 \\ b \end{smallmatrix}) \tag{31}$$

where $\mathbf{r}_0(\begin{smallmatrix} l \\ 0 \end{smallmatrix})$ and $\mathbf{r}_0(\begin{smallmatrix} 0 \\ b \end{smallmatrix})$ are the equilibrium positions of the l^{th} unit cell and b^{th} atom in the unit cell, respectively.

The allowed wavevectors are defined by

$$\boldsymbol{\kappa} = \sum_{\alpha} \mathbf{b}_\alpha \frac{n_\alpha}{N_\alpha} \tag{32}$$

where $\mathbf{b}_\alpha$ are the reciprocal lattice vectors,[4] which are related to the (Bravais) lattice vectors in Eq. 30, and $-N_\alpha/2 < n_\alpha \leq N_\alpha/2$, where n_α and N_α are even integers.[36] The reciprocal points are taken to be in the first BZ.[4]

Allowed Wavevectors in Disordered Materials

Strictly speaking, the only allowed wavector in a disordered system is the gamma point. As such, the lattice dynamics calculations are performed at the gamma point:

$$\omega^2(\begin{smallmatrix} \boldsymbol{\kappa} \\ \nu \end{smallmatrix})\, \mathbf{e}(\begin{smallmatrix} \boldsymbol{\kappa} \\ \nu \end{smallmatrix}) = D(\begin{smallmatrix} \boldsymbol{\kappa} \\ \nu \end{smallmatrix})\, \mathbf{e} \tag{33}$$

$$\omega^2\kappa = 0\mathbf{e}\kappa = 0 = D\kappa = 0\mathbf{e}\kappa = 0 \tag{34}$$

The modes analyzed at the gamma point are called Allen-Feldman (AF) type modes, which are non-propagating and referred to as "diffusons".

Howvere, even in a glass there is a finite sound speed (acoustic mode group velocity). For a disordered system, the group velocities at the -point are zero except for the three acoustic modes corresponding to $\omega = 0$. Thus, small but finite values of κ are required to analyze the phonon behavior in glasses and heavily disordered systems.

A Allen Feldman Calculation for Finite Wavectors

One advantage of studying the energy diffusivity instead of the thermal conductivity is that d is finite at nonzero frequency when evaluated at the harmonic level. By contrast, T is generally infinite if anharmonic corrections are ig- nored. This is because d in the integrand of Eq. 4 di- verges too strongly at low due to phonons that are progres- sively less scattered with increasing wavelength.[16]

In order to cure this divergence, additional scattering mechanisms, beyond harmonic theory, are typically invoked resulting in an additional contribution to the diffusivity, dc. Upon adding dc to the harmonic contribution, d, for example, as if they were two conductors in series 52, one obtains the total diffusivity dT, dT1 = d1 + dc1 , 22 Graebner, Golding, and Allen have demonstrated that the thermal conductivity of many glassy materials can be fitted by assuming an expression for dT consistent with Eq. 22 or more accurately its analog in terms of the mean-free-path 53. According to their analysis, the first contribution in Eq. 22, d, corresponds to a mean free path that ex- hibits a cross-over from Rayleigh law = 4 to a frequency-independent value min. The second low contri- bution, dc, arises from assuming resonant scattering and relaxational absorption of propagating phonons by two-level systems 11.

16

B Molecular dynamics simulations

Can take the expansion of the crystal energy and run F=ma.

B.1 Green-Kubo Method

The Green-Kubo method is an equilibrium molecular dynamics approach that relates the equilibrium fluctuations of the heat current vector, $\mathbf{S}$, to the thermal conductivity, k, via the fluctuation-dissipation theorem. The superlattice thermal conductivity in the l-th direction (either the cross-plane or in-plane direction) is given by[?]

$$k_l = \frac{1}{k_{\mathrm{B}} V T^2} \int_0^\infty \langle S_l(t) S_l(0) \rangle dt, \tag{35}$$

where t is time, V and T are the system volume and temperature, and S_l and $\langle S_l(t) S_l(0) \rangle$ are the l-th components of the heat current vector and the heat current autocorrelation function (HCACF).

There are multiple ways to define the heat current vector.[?,?,19] The most commonly used definition is

$$\mathbf{S}_1 = \frac{d}{dt}\sum_i \mathbf{r}_i E_i, \tag{36}$$

where E_i is the energy of atom i, and the summation is over all of the atoms in the system. In a solid, where there is no net atomic motion, the heat flux can also be written using the equilibrium positions ($\mathbf{r}_{i,o}$) as

$$\mathbf{S}_2 = \frac{d}{dt}\sum_i \mathbf{r}_{i,o} E_i. \tag{37}$$

The thermal conductivity predictions obtained using both definitions of the heat current vector were compared in my previous work.[?] While both definitions result in the same prediction for the thermal conductivity, the $\mathbf{S_2}$ definition was found to be preferable for solid-phase simulations. This definition is preferred because strong oscillations that are present in the HCACF when using the $\mathbf{S_1}$ definition are avoided. These oscillations were found to complicate the specification of the thermal conductivity in simulations of several different material systems.[?,8,23,24] An additional benefit is that the heat current vector is less computationally expensive with the $\mathbf{S_2}$ definition than the $\mathbf{S_1}$ definition [although not immediately obvious from Eqs. (36) and (37), the $\mathbf{S_1}$ definition requires the calculation of the potential energy of each atom while the $\mathbf{S_2}$ definition does not[?]]. All of the Green-Kubo results presented here were obtained using the $\mathbf{S_2}$ definition of the heat current vector.

C Derivation of Phonon Spectral Energy Density

To derive the correct expression for the phonon SED, Φ, we begin with harmonic lattice dynamics theory.[12,37] The derivation outlined here is presented in detail in Appendix C.

The system Hamiltonian, H, is[12]

$$\begin{aligned} H =& \frac{1}{2}\sum_{\boldsymbol{\kappa},\nu}^{N,3n} \left[\dot{q}^*(\tbinom{\boldsymbol{\kappa}}{\nu};t)\,\dot{q}(\tbinom{\boldsymbol{\kappa}}{\nu};t) + \omega_0^2(\tbinom{\boldsymbol{\kappa}}{\nu})\,q^*(\tbinom{\boldsymbol{\kappa}}{\nu};t)\,q(\tbinom{\boldsymbol{\kappa}}{\nu};t)\right] \\ =& \sum_{\boldsymbol{\kappa},\nu}^{N,3n} \left[T(\tbinom{\boldsymbol{\kappa}}{\nu};t) + V(\tbinom{\boldsymbol{\kappa}}{\nu};t)\right], \end{aligned} \tag{38}$$

where t is time, $\omega_0(\tbinom{\boldsymbol{\kappa}}{\nu})$ is the frequency of the phonon mode denoted by wave vector $\boldsymbol{\kappa}$ and dispersion branch ν, and N and n are the total number of unit cells and the number of atoms in the unit cell. The Hamiltonian is the total system energy and is the sum of the mode- and time-dependent kinetic and potential energies, $T(\tbinom{\boldsymbol{\kappa}}{\nu};t)$ and $V(\tbinom{\boldsymbol{\kappa}}{\nu};t)$.

The phonon normal mode coordinate[12] and its time derivative are given by

$$q(\substack{\boldsymbol{\kappa} \\ \nu};t) = \sum_{\alpha,b,l}^{3,n,N} \sqrt{\frac{m_b}{N}} u_\alpha(\substack{l \\ b};t)\, e^*(\substack{\boldsymbol{\kappa} & b \\ \nu & \alpha}) \exp[i\boldsymbol{\kappa}\cdot\mathbf{r}_0(\substack{l \\ 0})] \tag{39}$$

and

$$\dot{q}(\substack{\boldsymbol{\kappa} \\ \nu};t) = \sum_{\alpha,b,l}^{3,n,N} \sqrt{\frac{m_b}{N}} \dot{u}_\alpha(\substack{l \\ b};t)\, e^*(\substack{\boldsymbol{\kappa} & b \\ \nu & \alpha}) \exp[i\boldsymbol{\kappa}\cdot\mathbf{r}_0(\substack{l \\ 0})], \tag{40}$$

where m_b is the mass of the b^{th} atom in the unit cell and $\mathbf{r}_0(\substack{l \\ 0})$ is the equilibrium position vector of the l^{th} unit cell. The α-component of the displacement from equilibrium, $u_\alpha(\substack{l \\ b};t)$, and velocity, $\dot{u}_\alpha(\substack{l \\ b};t)$, of the b^{th} atom in the l^{th} unit cell are time-dependent and are related to the phonon mode coordinates through the time-independent eigenvector and that has components $e(\substack{\boldsymbol{\kappa} & b \\ \nu & \alpha})$.[12]

The expectation value of the kinetic energy of the normal mode is

$$\langle T(\substack{\boldsymbol{\kappa} \\ \nu})\rangle = \frac{1}{2}\lim_{\tau_0\to\infty}\frac{1}{\tau_0}\int_0^{\tau_0} \dot{q}^*(\substack{\boldsymbol{\kappa} \\ \nu};t)\,\dot{q}(\substack{\boldsymbol{\kappa} \\ \nu};t)\,dt. \tag{41}$$

The kinetic energy of the normal mode can be transformed from the time domain t to the frequency domain ω by Parseval's theorem,[29]

$$T(\substack{\boldsymbol{\kappa} \\ \nu};\omega) = \lim_{\tau_0\to\infty}\frac{1}{2\tau_0}\left|\frac{1}{\sqrt{2\pi}}\int_0^{\tau_0}\dot{q}(\substack{\boldsymbol{\kappa} \\ \nu};t)\exp(-i\omega t)dt\right|^2. \tag{42}$$

Following the derivation in Appendix C, one arrives at the expression for the phonon SED of a single phonon mode,

$$\Phi(\substack{\boldsymbol{\kappa} \\ \nu};\omega) = C_0(\substack{\boldsymbol{\kappa} \\ \nu})\,\frac{\Gamma(\substack{\boldsymbol{\kappa} \\ \nu})/\pi}{[\omega_0(\substack{\boldsymbol{\kappa} \\ \nu})-\omega]^2+\Gamma^2(\substack{\boldsymbol{\kappa} \\ \nu})}. \tag{43}$$

which is a Lorentzian function with center at $\omega_0(\substack{\boldsymbol{\kappa} \\ \nu})$ and a half-width at half-maximum (linewidth) of $\Gamma(\substack{\boldsymbol{\kappa} \\ \nu})$. We know from anharmonic lattice dynamics that the phonon linewdith is related to the phonon lifetime by[19,20]

$$\tau(\substack{\boldsymbol{\kappa} \\ \nu}) = \frac{1}{2\Gamma(\substack{\boldsymbol{\kappa} \\ \nu})}. \tag{44}$$

Since the MD simulations we perform here are classical, in the harmonic limit there is an equipartition of energy and $\sum_\nu^{3n} T(\substack{\boldsymbol{\kappa} \\ \nu};\omega) \approx \sum_\nu^{3n} V(\substack{\boldsymbol{\kappa} \\ \nu};\omega)$.[25] In an anharmonic system, equipartition of energy is a good approximation at low temperatures and can be tested by measuring the specific heat (Section C.2). Assuming equipartition of energy, the phonon SED at a particular wavevector is

$$\Phi(\omega,\boldsymbol{\kappa}) = 2\sum_\nu^{3n} T(\substack{\boldsymbol{\kappa} \\ \nu};\omega)\,, \tag{45}$$

which is a superposition of $3n$ Lorentzian functions,

$$\Phi(\omega,\boldsymbol{\kappa}) = \sum_{\nu}^{3n} C_0(\overset{\boldsymbol{\kappa}}{\nu}) \, \frac{\Gamma(\overset{\boldsymbol{\kappa}}{\nu}) \, / \pi}{[\omega_0(\overset{\boldsymbol{\kappa}}{\nu}) - \omega]^2 + \Gamma^2(\overset{\boldsymbol{\kappa}}{\nu})}, \tag{46}$$

with centers at $\omega_0(\overset{\boldsymbol{\kappa}}{\nu})$ for each polarization.

Φ is calculated using Eqs. (40) and (42), and is fit using Eq. (43). For simplicity, we refer to $\Phi(\omega,\boldsymbol{\kappa})$ as Φ. Previous work has used a time domain representation for the phonon mode energy, while Φ is represented in the frequency domain.[22,27,36] The time and frequency domain approaches are equivalent by use of the Wiener-Khinchin theorem.[27,29]

We start from Eq. (40). In an anharmonic system, the phonon populations fluctuate about the equilibrium distribution function.[37] The phonon mode coordinate for the mode described by $(\nu,\boldsymbol{\kappa})$ and its time derivative can be written as[12]

$$q(\overset{\boldsymbol{\kappa}}{\nu};t) = q_{SS}(\overset{\boldsymbol{\kappa}}{\nu};t) + q_T(\overset{\boldsymbol{\kappa}}{\nu};t) \tag{47}$$

and

$$\dot{q}(\overset{\boldsymbol{\kappa}}{\nu};t) = \dot{q}_{SS}(\overset{\boldsymbol{\kappa}}{\nu};t) + \dot{q}_T(\overset{\boldsymbol{\kappa}}{\nu};t) \, . \tag{48}$$

The steady-state (SS) and transient (T) parts and their time derivatives are given by

$$\begin{aligned} q_{SS}(\overset{\boldsymbol{\kappa}}{\nu};t) = & C_1(\overset{\boldsymbol{\kappa}}{\nu}) \exp[i\omega_0(\overset{\boldsymbol{\kappa}}{\nu}) \, t] \\ & + C_2(\overset{\boldsymbol{\kappa}}{\nu}) \exp[-i\omega_0(\overset{\boldsymbol{\kappa}}{\nu}) \, t], \end{aligned} \tag{49}$$

$$\begin{aligned} q_T(\overset{\boldsymbol{\kappa}}{\nu};t) = & \exp[-\Gamma(\overset{\boldsymbol{\kappa}}{\nu}) \, |t|] \{ C_3(\overset{\boldsymbol{\kappa}}{\nu}) \exp[i\omega_0(\overset{\boldsymbol{\kappa}}{\nu}) \, t] \\ & - C_4(\overset{\boldsymbol{\kappa}}{\nu}) \exp[-i\omega_0(\overset{\boldsymbol{\kappa}}{\nu}) \, t] \}, \end{aligned} \tag{50}$$

$$\dot{q}_{SS}(\overset{\boldsymbol{\kappa}}{\nu};t) = i\omega_0 \left\{ C_1(\overset{\boldsymbol{\kappa}}{\nu}) \exp[i\omega_0(\overset{\boldsymbol{\kappa}}{\nu}) \, t] - C_2(\overset{\boldsymbol{\kappa}}{\nu}) \exp[-i\omega_0(\overset{\boldsymbol{\kappa}}{\nu}) \, t] \right\}, \tag{51}$$

and

$$\begin{aligned} \dot{q}_T(\overset{\boldsymbol{\kappa}}{\nu};t) = & \exp[-\Gamma(\overset{\boldsymbol{\kappa}}{\nu}) \, |t|] \{ C_3(\overset{\boldsymbol{\kappa}}{\nu}) \left[i\omega_0(\overset{\boldsymbol{\kappa}}{\nu}) - \Gamma(\overset{\boldsymbol{\kappa}}{\nu}) \right] \exp[i\omega_0(\overset{\boldsymbol{\kappa}}{\nu}) \, t] \\ & - C_4(\overset{\boldsymbol{\kappa}}{\nu}) \left[i\omega_0(\overset{\boldsymbol{\kappa}}{\nu}) + \Gamma(\overset{\boldsymbol{\kappa}}{\nu}) \right] \exp[-i\omega_0(\overset{\boldsymbol{\kappa}}{\nu}) \, t] \} \, , \end{aligned} \tag{52}$$

where the Cs are constants and $\omega_0(\overset{\boldsymbol{\kappa}}{\nu})$ and $\Gamma(\overset{\boldsymbol{\kappa}}{\nu})$ are the phonon mode frequency and scattering rate (i.e., linewidth). The transient part describes the creation of an excess in the population of a phonon mode for $t < 0$ and its decay back to equilibrium for $t > 0$.

Phonon interactions arise due to anharmonicity, which causes fluctuations in the phonon populations. These population fluctuations are commonly modeled using the excitation and decay of a single phonon mode (single mode relaxation time approximation).[22,37] In a real

system, there will be multiple phonons in each mode that simultaneously grow or decay with time. Thus, dealing only with $\dot{q}$, we let

$$\begin{aligned}\dot{q}(\boldsymbol{\kappa}_\nu;t) = &\sum_j i\exp[-\Gamma(\boldsymbol{\kappa}_\nu)\,|t-t_j|]\times \\ &\{A_j(\boldsymbol{\kappa}_\nu)\,[\omega_0(\boldsymbol{\kappa}_\nu)+i\Gamma(\boldsymbol{\kappa}_\nu)]\exp[i\omega_0(\boldsymbol{\kappa}_\nu)\,(t-t_j)] \\ &- B_j(\boldsymbol{\kappa}_\nu)\,[\omega_0(\boldsymbol{\kappa}_\nu)-i\Gamma(\boldsymbol{\kappa}_\nu)]\exp[-i\omega_0(\boldsymbol{\kappa}_\nu)\,(t-t_j)]\} \\ &,\end{aligned} \tag{53}$$

where many phonons in each mode, indexed by j, are simultaneously being created and destroyed. The phonons grow for $t < t_j$ and decay for $t > t_j$ and A_j and B_j are constants. We are not concerned with the values of t_j, A_j, and B_j, though they should satisfy the long-time average $\langle \dot{q}^*_{SS}(\boldsymbol{\kappa}_\nu;t)\,\dot{q}_{SS}(\boldsymbol{\kappa}_\nu;t)\rangle = \langle \dot{q}^*(\boldsymbol{\kappa}_\nu;t)\,\dot{q}(\boldsymbol{\kappa}_\nu;t)\rangle$.

The expectation value of the kinetic energy of the normal coordinate is

$$\langle T(\boldsymbol{\kappa}_\nu)\rangle = \frac{1}{2}\lim_{\tau_0\to\infty}\frac{1}{\tau_0}\int_0^{\tau_0}\dot{q}^*(\boldsymbol{\kappa}_\nu;t)\,\dot{q}(\boldsymbol{\kappa}_\nu;t)\,dt. \tag{54}$$

This expression can be transformed from the time domain t to the frequency domain ω by Parseval's theorem,[29] allowing Eq. (54) to be written as

$$T(\boldsymbol{\kappa}_\nu;\omega) = \lim_{\tau_0\to\infty}\frac{1}{2\tau_0}\left|\frac{1}{\sqrt{2\pi}}\int_0^{\tau_0}\dot{q}(\boldsymbol{\kappa}_\nu;t)\exp(-i\omega t)dt\right|^2. \tag{55}$$

By substituting Eq. (53) into Eq. (55) and performing the integration over time we find

$$\begin{aligned}T(\boldsymbol{\kappa}_\nu;\omega) = \frac{1}{16\pi\tau_0}\Bigg|\sum_j \exp[-i\omega t_j]\Bigg\{&A_j(\boldsymbol{\kappa}_\nu)\,\frac{\omega_0(\boldsymbol{\kappa}_\nu)+i\Gamma(\boldsymbol{\kappa}_\nu)}{\omega_0(\boldsymbol{\kappa}_\nu)-\omega+i\Gamma(\boldsymbol{\kappa}_\nu)} \\ &+B_j(\boldsymbol{\kappa}_\nu)\,\frac{\omega_0(\boldsymbol{\kappa}_\nu)-i\Gamma(\boldsymbol{\kappa}_\nu)}{\omega_0(\boldsymbol{\kappa}_\nu)+\omega-i\Gamma(\boldsymbol{\kappa}_\nu)}\Bigg\}\Bigg|^2.\end{aligned} \tag{56}$$

We are primarily interested in values of ω where $\omega \approx \omega_0$ when $\Gamma << \omega_0$ (this condition is met for the three systems studied here). When $\omega \approx \omega_0$, the term involving A_j becomes large and the term involving B_j can be neglected (alternatively, we could ignore the term involving A_j when $\omega \approx -\omega_0$). Hence, we find

$$\begin{aligned}T(\boldsymbol{\kappa}_\nu;\omega) = \frac{1}{16\pi\tau_0}\sum_j\sum_{j'}&\cos\left[\omega(t_{j'}-t_j)\right]A_j(\boldsymbol{\kappa}_\nu)\,A_{j'}(\boldsymbol{\kappa}_\nu) \\ &\times\frac{\omega_0^2(\boldsymbol{\kappa}_\nu)+\Gamma^2(\boldsymbol{\kappa}_\nu)}{\Gamma(\boldsymbol{\kappa}_\nu)}\,\frac{\Gamma(\boldsymbol{\kappa}_\nu)}{[\omega_0(\boldsymbol{\kappa}_\nu)-\omega]^2+\Gamma^2(\boldsymbol{\kappa}_\nu)}.\end{aligned} \tag{57}$$

We arrive at the expression for the phonon spectral energy density by summing Eq. (57)

$$\Phi(\omega,\boldsymbol{\kappa}) = 2\sum_\nu^{3n}T(\boldsymbol{\kappa}_\nu;\omega) = \sum_\nu^{3n}C_0(\boldsymbol{\kappa}_\nu)\,\frac{\Gamma(\boldsymbol{\kappa}_\nu)/\pi}{[\omega_0(\boldsymbol{\kappa}_\nu)-\omega]^2+\Gamma^2(\boldsymbol{\kappa}_\nu)}, \tag{58}$$

where the factor of two comes from equipartition of kinetic and potential energy (valid for a harmonic classical system, see Section C.2), and

$$C_0(\boldsymbol{\kappa}_\nu) = \sum_j \sum_{j'} \cos\left[\omega(t_{j'} - t_j)\right] A_j(\boldsymbol{\kappa}_\nu)\, A_{j'}(\boldsymbol{\kappa}_\nu)\, \frac{\omega_0^2(\boldsymbol{\kappa}_\nu) + \Gamma^2(\boldsymbol{\kappa}_\nu)}{8\tau_0 \Gamma(\boldsymbol{\kappa}_\nu)}. \tag{59}$$

Thus, the phonon spectral energy density $\Phi(\omega, \boldsymbol{\kappa})$ is a superposition of $3n$ Lorentzian functions with centers at $\omega_0(\boldsymbol{\kappa}_\nu)$ (one for each polarization) with a half-width at half-maximum of $\Gamma(\boldsymbol{\kappa}_\nu)$. Φ is a spectral energy density since its integral over all wavevectors and frequencies is the total crystal energy. The Hamiltonian can be written as

$$H = \int_{V_{BZ}} \int_0^\infty \Phi(\omega, \boldsymbol{\kappa}) d\omega d\boldsymbol{\kappa}, \tag{60}$$

where V_{BZ} is the volume of the Brioullin zone. Like the broadening in frequency, there is also a broadening of the SED in wavevector.[35] For a finite sampling of the Brioullin zone, the Hamiltonian can be written approximately as

$$H \approx \sum_{\boldsymbol{\kappa}}^{N} \int_{-\infty}^{\infty} \Phi(\omega, \boldsymbol{\kappa}) d\omega = 2 \sum_{\boldsymbol{\kappa},\nu}^{N,3n} \langle T(\boldsymbol{\kappa}_\nu; t) \rangle. \tag{61}$$

C.1 Thermal Conductivity

Once the frequencies and lifetimes of all phonon modes in the Brillouin zone are obtained, the bulk thermal conductivity in direction $\mathbf{n}$, $k_\mathbf{n}$, can be calculated from[40]

$$k_\mathbf{n} = \sum_{\boldsymbol{\kappa}} \sum_{\nu} c_{ph}(\boldsymbol{\kappa}_\nu)\, v_{g,\mathbf{n}}^2(\boldsymbol{\kappa}_\nu)\, \tau(\boldsymbol{\kappa}_\nu)\,. \tag{62}$$

Here, c_{ph} is the phonon volumetric specific heat and $v_{g,\mathbf{n}}$ is the component of the group velocity vector in direction $\mathbf{n}$. Since the systems we consider are classical and obey Maxwell-Boltzmann statistics,[25] the specific heat is k_B/V per mode in the harmonic limit where V is the system volume. This approximation is used here and has been shown to be suitable for LJ argon[22] and SW silicon.[15] The group velocity vector is the gradient of the dispersion curves (i.e., $\partial\omega/\partial\boldsymbol{\kappa}$), which can be calculated from the frequencies and wavevectors using finite differences. In this work, the group velocities are calculated using finite difference and quasi-harmonic lattice dynamics because a very small finite difference can be used which reduces the error.[21] To predict a bulk thermal conductivity, it is necessary to perform a finite simulation size scaling procedure as discussed in Appendix **??**.

C.2 Computational Cost

The computational cost of evaluating Eq. (**??**) is less than that for Eq. (42) by a factor of $3b$, where b is the number of atoms in the unit cell. For bulk crystals, the number of atoms in the unit cell is typically small ($b < 10$). In the CNT system, $b = 32$ and evaluating Φ' is two orders of magnitude less expensive than evaluating Φ.

To calculate the phonon lifetimes, the MD simulation time should be an order of magnitude longer than the longest phonon lifetime.[33] If only the phonon frequencies are required, however, the location of the peaks in Φ and Φ' develop in a time on the order of the inverse of the phonon frequency, $1/\omega_0(\kappa_\nu)$. For the systems studied here, this time to develop the peak locations can be two to five orders of magnitude less than the time needed to develop the lifetimes.

Fitting Φ' fitting becomes challenging at higher temperatures when the phonon linewidths broaden to become comparable to the spacing between mode frequencies. The cost of fitting Φ' can be reduced by fitting the peaks from all allowed wavevectors in the system simultaneously, but the error associated with this procedure is unknown.[31] We find that a semi-automated procedure, whereby the fits are visualized, is necessary to ensure that all peaks are fit correctly. While the computational cost of fitting Φ' is much smaller than the computational cost of calculating Φ', the semi-automated fitting procedure can be of similar time cost to the user. The cost of fitting Φ is much smaller because the different polarization peaks can be isolated and the fitting can be fully automated.

D Computational Cost

D.1 Harmonic and Anharmonic Lattice Dynamics Calculations of Large Unit Cells

$cost_{Si} = 1 supercell Force calculation/min$

Naive Compuational Algorithm for harmonic

$for i = 1 : NUM_ATOMS_UCELL for j = i : NUM_ATOMS_UCELL LD.Phi(i,j) = dUdr(LD.LJ.r(i), LD.LJ.r(j)) end end$

scale as b^2

These references suggest Lattice Dynamics calculations are expensive. This is true for Anharmonic Lattice Dynamics calcalculations, which scale with b^3. For large unit cell materials, this is expensive.

Naive Compuational Algorithm for anharmonic

$for i = 1 : NUM_ATOMS_UCELL for j = i : NUM_ATOMS_UCELL for k = j : NUM_ATOMS_UCELL$
$dUdr(LD.LJ.r(i), LD.LJ.r(j), LD.LJ.r(k)) end end end$

$cost = b^3$

Both of these calculations can be reduced by recognition of crystal symmetries. For LUC, there are no symmetries to recognize (in general).

A. Ward, D. A. Broido, D. A. Stewart and G. Deinzer, Ab initio theory of the lattice thermal conductivity in diamond, Phys. Rev. B: Condens. Matter Mater. Phys., 2009, 80, 125203. A. Ward and D. A. Broido, Intrinsic phonon relaxation times from first principle studies of the thermal conductivity of Si and Ge, Phys. Rev. B: Condens. Matter Mater. Phys., 2010, 81, 085205. J. An, A. Subedi and D. J. Singh, Ab initio phonon dispersions for PbTe, Solid State Commun., 2008, 148, 417419. J. Dong, O. F. Sankey and C. W. Myles, Theoretical study of the lattice thermal conductivity in Ge framework semiconductors, Phys. Rev. Lett., 2001, 86, 2361. N. de Koker, Thermal conductivity of MgO periclase from equilibrium first principles molecular dynamics, Phys. Rev. Lett., 2009, 103, 125902. N. Bernstein, J. L. Feldman and D. J. Singh, Calculations of dynamical properties of skutterudites: Thermal conductivity, thermal expansivity, and atomic mean-square displacement, Phys. Rev. B: Condens. Matter Mater. Phys., 2010, 81, 134301.

E Role of Anharmonicity

a) can you just run a harmonic FC MD to measure the conductivity?

AF Calculation: Harmonic, Gamma Point Only

NMD Calculation: AnHarmonic, "allowed" wavevectors

Harmonic FC MD Calculation Amorphous/Alloy: Harmonic, "allowed" wavevectors

Implications for LUC

Later Work: AnHarmonic FC Calculation: AnHarmonic, "allowed" wavevectors

Later Work: Gruneisen parameter for Disordered system: can this characterize the behavior of acoustic phonons, which may scale like Umklapp, as oppposed to the Cahill model.

w (q,L+dL) - w(q,L-dL) / 2w(q) (L/2dL)

This process can be approximated by Klemens expression for anharmonic phonon scattering.15

where is the Grneisen parameter, M the mass of the unit cell, and ,max the maximum frequency of branch . The Grneisen parameter at each q and can be calculated from the change in the phonons frequencies with the cell volume.

The importance of the Umklapp scattering effect in skutteru- dites due to the cubic anharmonic interaction between filler and host atoms, has recently been discussed by Bernstein

et al.16

References

[1]

[2]

[3] Philip B. Allen and Joseph L. Feldman. Thermal conductivity of disordered harmonic solids. *Physical Review B*, 48(17):12581–12588, Nov 1993.

[4] N. W. Ashcroft and N. D. Mermin. *Solid State Physics*. Saunders, Fort Worth, 1976.

[5] D. G. Cahill, S. K. Watson, and R. O. Pohl. Lower limit to thermal conductivity of disordered crystals. *Physical Review B*, 46:6131–6140, 1992.

[6] David G. Cahill and R. O. Pohl. Thermal conductivity of amorphous solids above the plateau. *Physical Review B*, 35:40674073, 1987.

[7] David G. Cahill, S. K. Watson, and R. O. Pohl. Lower limit to the thermal conductivity of disordered crystals. *Phys. Rev. B*, 46:6131–6140, Sep 1992.

[8] J. Che, T. Cagin, W. Deng, and W. A. Goddard III. Thermal conductivity of diamond and related materials from molecular dynamics simulations. *Journal of Chemical Physics*, 113:6888–6900, 2000.

[9] G Chen, M S Dresselhaus, G Dresselhaus, J Fleurial, and T Caillat. Recent developments in thermoelectric materials. *International Materials Reviews*, 48(1):45–66, 2003.

[10] Mogens Christensen, Nina Lock, Jacob Overgaard, and Bo B. Iversen. Crystal structures of thermoelectric n- and p-type ba8ga16ge30 studied by single crystal, multitemperature, neutron diffraction, conventional x-ray diffraction and resonant synchrotron x-ray diffraction. *Journal of the American Chemical Society*, 128(49):15657–15665, 2006.

[11] J. L. Cohn, G. S. Nolas, V. Fessatidis, T. H. Metcalf, and G. A. Slack. Glasslike heat conduction in high-mobility crystalline semiconductors. *Phys. Rev. Lett.*, 82:779–782, Jan 1999.

[12] M. T. Dove. *Introduction to Lattice Dynamics*. Cambridge, Cambridge, 1993.

[13] M.?S. Dresselhaus, G. Chen, M.?Y. Tang, R.?G. Yang, H. Lee, D.?Z. Wang, Z.?F. Ren, J.-P. Fleurial, and P. Gogna. New directions for low-dimensional thermoelectric materials. *Advanced Materials*, 19(8):1043–1053, 2007.

[14] J. J. Freeman and A. C. Anderson. Thermal conductivity of amorphous solids. *Physical Review B*, 34:56845690, 1986.

[15] J. V. Goicochea, M. Madrid, and C. H. Amon. Thermal properties for bulk silicon based on the determination of relaxation times using molecular dynamics. *Journal of Heat Transfer*, 132:012401, 2010.

[16] J. E. Graebner, B. Golding, and L. C. Allen. Phonon localization in glasses. *Phys. Rev. B*, 34:5696–5701, Oct 1986.

[17] Tao He, Jiazhong Chen, H. David Rosenfeld, and M. A. Subramanian. Thermoelectric properties of indium-filled skutterudites. *Chemistry of Materials*, 18(3):759–762, 2006.

[18] M. Kaviany. *Heat Transfer Physics*. Cambridge University Press, New York, 2008.

[19] A. J. C. Ladd, B. Moran, and W. G. Hoover. Lattice thermal conductivity: A comparison of molecular dynamics and anharmonic lattice dynamics. *Physical Review B*, 34:5058–5064, 1986.

[20] A. A. Maradudin and A. E. Fein. Scattering of neutrons by an anharmonic crystal. *Physical Review*, 128:2589–2608, 1962.

[21] A. J. H. McGaughey, M. I. Hussein, E. S. Landry, M. Kaviany, and G. M. Hulbert. Phonon band structure and thermal transport correlation in a layered diatomic crystal. *Physical Review B*, 74:104304, 2006.

[22] A. J. H. McGaughey and M. Kaviany. Quantitative validation of the Boltzmann transport equation phonon thermal conductivity model under the single-mode relaxation time approximation. *Physical Review B*, 69:094303, 2004.

[23] A. J. H. McGaughey and M. Kaviany. Thermal conductivity decomposition and analysis using molecular dynamics simulations. Part II. Complex silica structures. *International Journal of Heat and Mass Transfer*, 47:1799–1816, 2004.

[24] A. J. H. McGaughey and J. Li. Molecular dynamics prediction of the thermal resistance of solid–solid interfaces in superlattices. In *Proceedings of IMECE 2006*. ASME, 2006. Paper number IMECE2006-13590.

[25] D. A. McQuarrie. *Statistical Mechanics*. University Science Books, Sausalito, 2000.

[26] A. J. Minnich, M. S. Dresselhaus, Z. F. Ren, and G. Chen. Bulk nanostructured thermoelectric materials: current research and future prospects. *Energy Environ. Sci.*, 2:–, 2009.

[27] Zhun-Yong Ong, Eric Pop, and Junichiro Shiomi. Reduction of phonon lifetimes and thermal conductivity of a carbon nanotube on amorphous silica. *Physical Review B*, 84(16):165418, 2011.

[28] P. F. Qiu, J. Yang, R. H. Liu, X. Shi, X. Y. Huang, G. J. Snyder, W. Zhang, and L. D. Chen. High-temperature electrical and thermal transport properties of fully filled skutterudites rfe[sub 4]sb[sub 12] (r = ca, sr, ba, la, ce, pr, nd, eu, and yb). *Journal of Applied Physics*, 109(6):063713, 2011.

[29] W. Rudin. *Real and Complex Analysis*. McGraw-Hill, New York, 1987.

[30] Brian C Sales, B C Chakoumakos, David Mandrus, and J W Sharp. Atomic displacement parameters and the lattice thermal conductivity of clathrate-like thermoelectric compounds. *Journal of Solid State Chemistry*, 146(2):528–532, 1999.

[31] Junichiro Shiomi, Keivan Esfarjani, and Gang Chen. Thermal conductivity of half-heusler compounds from first-principles calculations. *Physical Review B*, 84(10):125209, 2011.

[32] E. F. Steigmeier and I. Kudman. Acoustical-optical phonon scattering in ge, si, and iii-v compounds. *Phys. Rev.*, 141:767–774, Jan 1966.

[33] J. A. Thomas. *water flow and thermal transport through carbon nanotubes*. PhD Thesis, Carnegie Mellon University, Pittsburgh, PA, 2010.

[34] Eric S. Toberer, Alex Zevalkink, and G. Jeffrey Snyder. Phonon engineering through crystal chemistry. *J. Mater. Chem.*, 21:–, 2011.

[35] J. E. Turney. *Predicting phonon properties and thermal conductivity using anharmonic lattice dynamics calculations*. PhD Thesis, Carnegie Mellon University, Pittsburgh, PA, 2009.

[36] J. E. Turney, E. S. Landry, A. J. H. McGaughey, and C. H. Amon. Predicting phonon properties and thermal conductivity from anharmonic lattice dynamics calculations and molecular dynamics simulations. *Physical Review B*, 79:064301, 2009.

[37] D. C. Wallace. *Thermodynamics of Crystals*. Cambridge Univ. Press, Cambridge, UK, 1972.

[38] Xiao-Jun Wang, Mei-Bo Tang, Jing-Tai Zhao, Hao-Hong Chen, and Xin-Xin Yang. Thermoelectric properties and electronic structure of zintl compound bazn[sub 2]sb[sub 2]. *Applied Physics Letters*, 90(23):232107, 2007.

[39] Junyou Yang, Yuehua Chen, Wen Zhu, Jiangying Peng, Siqian Bao, Xi?an Fan, Xingkai Duan, and Anonymous. Effect of la filling on thermoelectric properties of laxco3.6ni0.4sb12-filled skutterudite prepared by ma-hp method. *Journal of Solid State Chemistry*, 179(1):212–216, 2006.

[40] J. M. Ziman. *Electrons and Phonons*. Oxford, New York, 2001.